Mathematical models of diffusion-constrained polymerase chain reactions: basis of high-throughput nucleic acid assays and simple self-organizing systems

John Aach and George M. Church*

FULL COLOR VERSIONS OF FIGURES

Department of Genetics and Lipper Center for Computational Genetics, Harvard Medical School,
77 Avenue Louis Pasteur, Boston, MA, 02115, USA

* to whom correspondence should be addressed

Harvard Medical School Department of Genetics
New Research Building, Rm 238
77 Avenue Louis Pasteur, Boston, MA 02115, USA
Email: http://arep.med.harvard.edu/gmc/email.html
Phone: (617) 432-1278
Fax: (617) 432-6513

January 29, 2004

(contains proof corrections)

The figures in this article, published in the *Journal of Theoretical Biology*, were rendered as gray scale images in the printed version of the journal, but in their original full color in the on line version. This document contains downloadable versions of the full color figures for readers who only have access to the printed version.

FIGURE LEGENDS

Figure 1

Polonies and polony generation. (a) Figurative illustration of polony generation showing interactions of molecular species in a polony gel during a single PCR cycle. After a denaturing cycle (first frame) only single-stranded DNA species are present in a gel: P = tethered primer (short black arrows), Q = untethered (free) primer (short blue arrows), S = untethered (free) strand (long blue arrows), T = tethered strand (long black arrows) (see Table 1 for notation and nomenclature). Arrows indicate 5'-to-3' orientation. Black circles indicate chemical anchoring of tethered species to gel matrix. Only untethered species (blue) are able to diffuse. During the annealing cycle, these untethered species continue to diffuse until they are captured by complementary tethered strands. Therefore, after annealing (second frame) a diffusing S strand has been captured by a tethered P primer, and a diffusing Q primer has been captured by a tethered T strand (indicated in boxes). After the subsequent replication phase (third frame), the captured P primer has extended to a T strand, and the captured Q primer has extended to an S strand, resulting in two ST molecules. These ST molecules will dissociate and the S strands will diffuse away in the following denaturing phase. (b) Image of actual polonies generated by protocol described in the text and illustrated in (a). Each colored spot is the product of the diffusion-constrained PCR amplification protocol generated by a single DNA template molecule. A mixture of two distinct templates was used in this reaction. Polonies were visualized by hybridizing primers specific to the two templates and extending with a single fluorescently labeled base which was different for the two templates, thereby labeling the two different kinds of polonies generated with different colors. Arrows indicate nearby polonies that have apparently deformed against each other rather than interpenetrate, illustrating the polony exclusion phenomenon (see text). Figure 1b copied from (Mitra, et al., 2003) by permission of publisher (see Acknowledgements).

Figure 2

Single polony growth and two polony interaction models. Each table describes the chemical reactions and the mathematical equations used to describe a PCR cycle. Each cycle comprises a series of three phases: denaturing, annealing, and replication. (a) Single polony growth model. The complete set of reactions and equations is described. (b) Two polony interaction model, described as a set of additions and changes to the single polony growth model. Note that diffusion equation boundary conditions are always as follows: S and U are 0 at the boundary of solution space. Q is always eQ (see Table 2) at the boundary of solution space (see text).

Figure 3

Results of a 3D SPGM simulation using standard parameters (Table 2) that illustrate key features of polony morphology and development. Each graph displays the concentration of a molecular species as a function of distance from the origin (radius), which is the location of the original polony template strand seed molecule, at the end of a particular phase of each of the 40 PCR cycles. Shown are P, Q, S, and T at the end of PCR denaturing phases, and PS and QT after PCR annealing phases. Axis labels are indicated on the P graph. The solid lines in each graph are the concentration curves for cycles 10, 20, 30, and 40. Concentrations are in units of molecules/μm^3. See text for details (Results).

Figure 4

Analysis of estimated polony yield by cycle. (a) Graph of $\log_{10}$ yield of S (logS) and T (logT) after every denaturing cycle from a 3D SPGM simulation with standard parameters (Table 2) except for being carried out to 100 cycles. Also shown (logT(reg)) is the graph of the regression of logT described by equation (1) in the text. In this regression, the cycle at which yield switched from exponential to power law growth was 23.3 (indicated by the vertical dashed line). The power law exponent was 4.3. (b) Evolution of power law exponent for logT as determined by

power law regressions over windows of 10 consecutive $\log_{10}$ T yields, showing gradual decline of power law exponents moving towards apparent asymptotes that depend on dimension. The 3D curve is the evolution of the power law exponent for the 3D simulation shown in (a). The 2D curves are power law exponent curves for 2D simulations of with standard parameters (Table 2) for gels that are 1 μm thick (2D.1μm) and 10 μm thick (2D.10μm). The 1D simulation assumes a 1D linear gel with a 1 μm^2 cross section (Table 2).

Figure 5

Polony interaction simulation illustrating the polony 'exclusion' phenomenon. Graphs show results from the end of the denaturing phase of cycle 40 from a 3D TPIM simulation using standard parameters (Table 2) that began with single ST and UV seed molecules at +12 and -12 μm from the origin along the Z-axis. See text for details. (a) and (b): Filled contour plots showing concentrations of tethered strands T (a) and V (b). (c) and (d): Contour plots showing overlays of T and V (c) and overlays of corresponding free strands S and U (d). (e) Scanner view (see text) of interacting T and V polonies, generated by computationally rotating, projecting, and integrating the concentration data of (c), that may be compared with scanned images of actual polonies obtained by fluorescence microscopy (Figure 1b). T density is indicated by red, V by green. (f): Comparison of T from this TPIM simulation with T from a corresponding SPGM simulation, where there is no interaction with another polony. (g) Corresponding comparison of S from this TPIM and the corresponding SPGM simulation. Arrowheads: see text. x: Maximum concentration (a-d). + (magenta) : location of initial polony seed molecule.

Figure 6

Polony interaction simulation illustrating the polony invasion phenomenon. Graphs show results from the end of the denaturing phase of cycle 40 from a 3D TPIM simulation using standard

parameters (Table 2) that began with single ST and UV seed molecules at +4 and –4 μm from the origin along the Z-axis. See text for details and Figure 5 for figure layout and notation.

Figure 7

Polony exclusion and invasion in two dimensions (a and b) and one dimension (c and d). (a) T concentration at end of denaturing phase of cycle 40 for 2D TPIM simulation of a 10 μm thick gel (Table 2) with polony seed molecules for ST and UV at +/-4 μm on the Y axis (indicated by magenta + signs). T concentration profile shows complex invasion geometry similar to 3D invasion geometry of Figure 6a. (b) Scanner view of T and V polonies from simulation in (a) shows merging along the midline similar to Figure 6e (arrow). (c) S, T, U, and V concentrations at end of denaturing phase of cycle 40 for 1D TPIM simulation (Table 2) with polony seed molecules ST and UV at +/-10μm, showing well-defined exclusion of polonies. T density is indicated by red, V by green. (d) Same variables as in (c) for 1D TPIM simulation with polony seeds at +/-4μm, showing polony invasion with 'tunneling' described in text (compare arrows in (d) and (c)). + (magenta): polony seed locations.

Figure 8

Measures of the extent of polony invasion in 3D TPIM simulations. Two measures are shown as functions of polony seed distance from the origin (in μm) and PCR cycle, and are based on concentration profiles and yields of tethered strand T after denaturing phases. Blue lines show each measure as a function of seed distance from origin at PCR cycle 40, the last cycle for standard simulations (Table 2). (a) FLTY measures the fractional loss in T yield due to the presence of a neighboring polony compared to an SPGM simulation in which the T polony develops without interference. (b) VVT is the total amount of V, the tethered strand of a

neighboring invading polony, divided by the total of the amounts of V and T, in the half space owned by the T polony.

Figure 1a

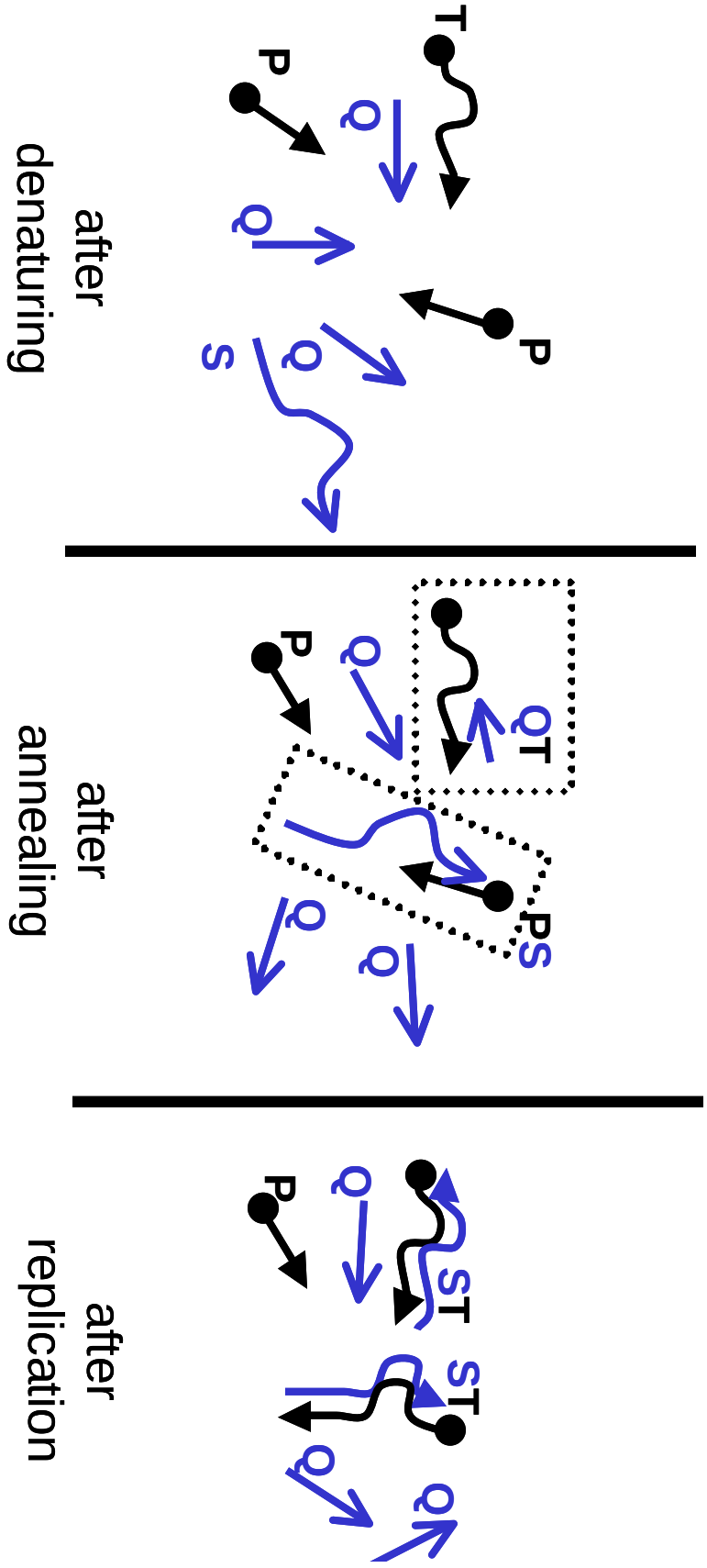
after denaturing
after annealing
after replication
T
P
P
S
T
PS
ST
ST

Figure 1b

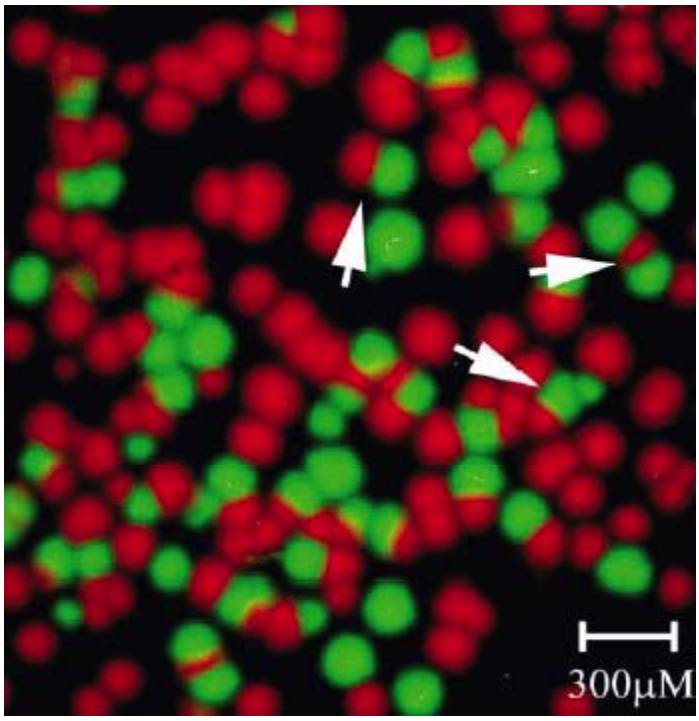

Figure 2 (a)

SINGLE POLONY GROWTH MODEL (SPGM)

DENATURING	ANNEALING	REPLICATION
	Reactions	
$ST \rightarrow S + T$	$P + S \xrightarrow{k_{PS}} PS$ $Q + T \xrightarrow{k_{QT}} QT$ $S + T \xrightarrow{k_{ST}} ST$	$PS \rightarrow ST$ $QT \rightarrow ST$
	Equations	
First moment: At all points in space $S \leftarrow S + ST$ $T \leftarrow T + ST$ $ST \leftarrow 0$ Rest of phase: $\frac{\partial Q}{\partial t} = D_Q \nabla^2 Q$ $\frac{\partial S}{\partial t} = D_S \nabla^2 S$	$\frac{\partial P}{\partial t} = -k_{PS} P \cdot S$ (A1) $\frac{\partial Q}{\partial t} = -k_{QT} Q \cdot T + D_Q \nabla^2 Q$ (A2) $\frac{\partial S}{\partial t} = -k_{PS} P \cdot S - k_{ST} S \cdot T + D_S \nabla^2 S$ $\frac{\partial T}{\partial t} = -k_{QT} Q \cdot T - k_{ST} S \cdot T$ $\frac{\partial PS}{\partial t} = k_{PS} P \cdot S$ $\frac{\partial QT}{\partial t} = k_{QT} Q \cdot T$ $\frac{\partial ST}{\partial t} = k_{ST} S \cdot T$	At all points in space $ST \leftarrow PS + QT + ST$ $QT \leftarrow 0$ $PS \leftarrow 0$

Figure 2 (b)

TWO POLONY INTERACTION MODEL (TPIM)

DENATURING	ANNEALING	REPLICATION
	Reactions	
Add reaction	Add reactions	Add reactions
$UV \rightarrow U + V$	$P + U \xrightarrow{k_{PU}} PU$ $Q + V \xrightarrow{k_{QV}} QV$ $U + V \xrightarrow{k_{UV}} UV$	$PU \rightarrow UV$ $QV \rightarrow UV$
	Equations	
Add equations	Replace equations (A1) and (A2) with	Add equations
First moment:	$\frac{\partial P}{\partial t} = -k_{PS} P \cdot S - k_{PU} P \cdot U$ $\frac{\partial Q}{\partial t} = -k_{QT} Q \cdot T - k_{QV} Q \cdot V + D_Q \nabla^2 Q$	At all points in space
At all points in space	Add equations	$UV \leftarrow PU + QV + UV$ $QV \leftarrow 0$ $PU \leftarrow 0$
$U \leftarrow U + UV$ $V \leftarrow V + UV$ $UV \leftarrow 0$	$\frac{\partial U}{\partial t} = -k_{PU} P \cdot U - k_{UV} U \cdot V + D_U \nabla^2 U$ $\frac{\partial V}{\partial t} = -k_{QV} Q \cdot V - k_{UV} U \cdot V$ $\frac{\partial PU}{\partial t} = k_{PU} P \cdot U$ $\frac{\partial QV}{\partial t} = k_{QV} Q \cdot V$ $\frac{\partial UV}{\partial t} = k_{UV} U \cdot V$	
Rest of phase:		
$\frac{\partial U}{\partial t} = D_U \nabla^2 U$		

Figure 3

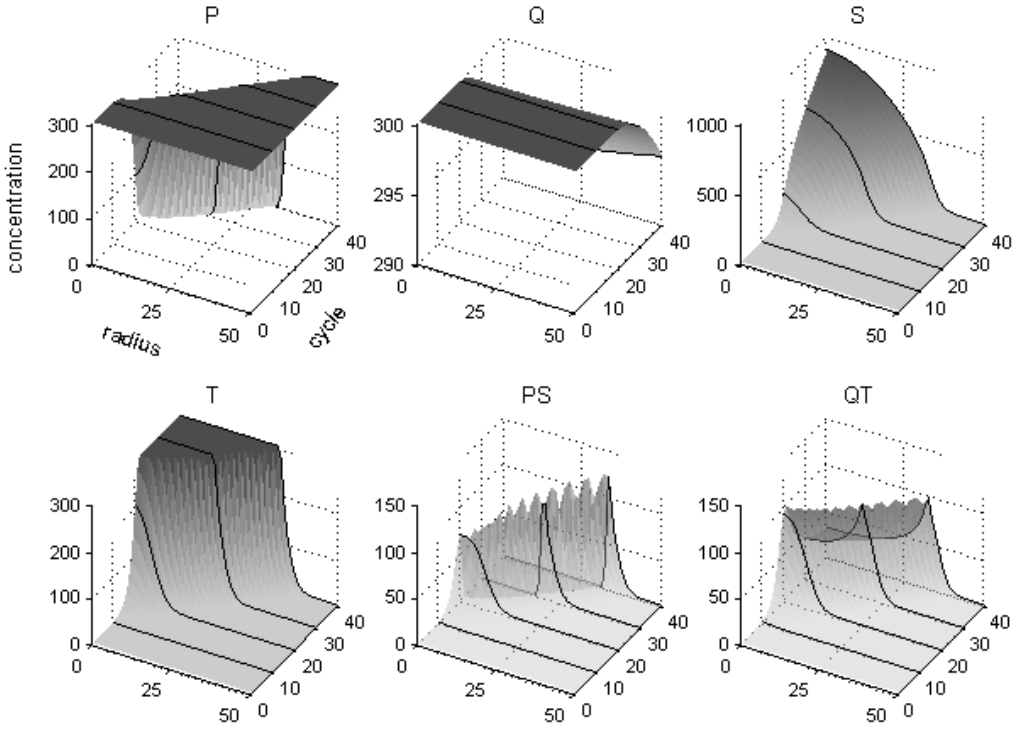
P
Q
S
T
PS
QT
concentration
radius
cycle
300
200
100
0
295
290
1000
500
150
50
0
25
50
10
20
30
40

Figure 4a

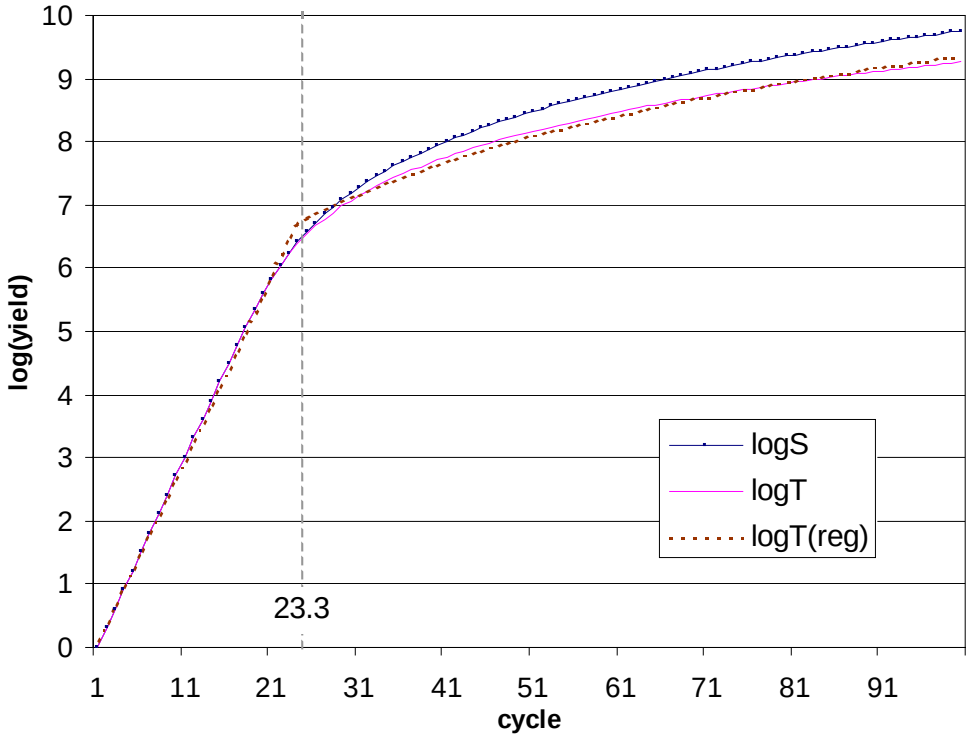

Figure 4b

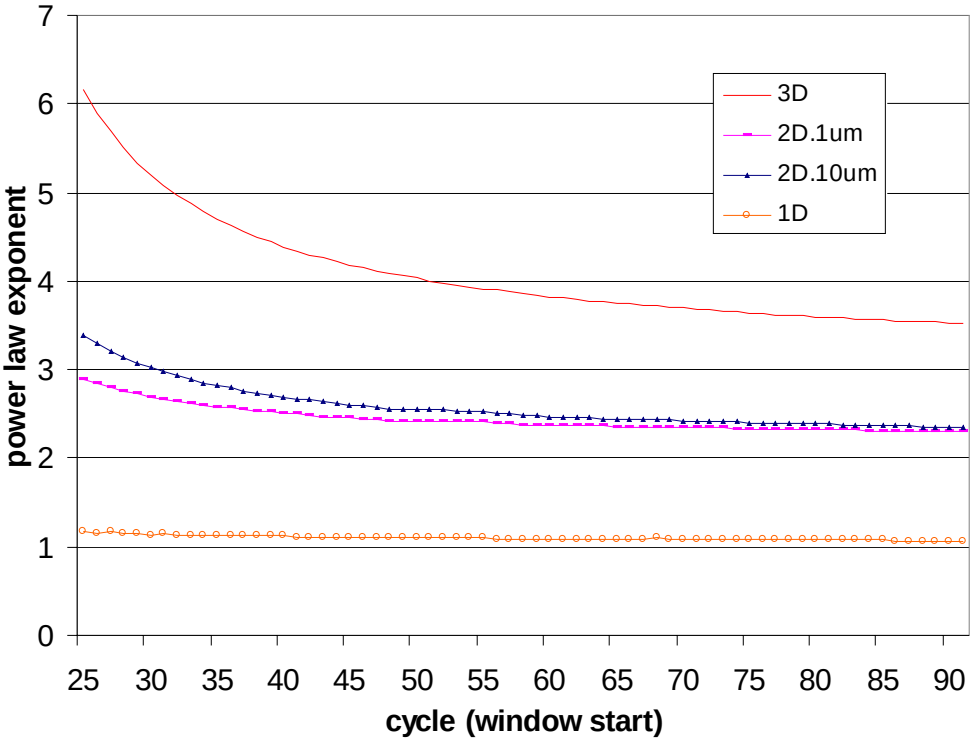

Figure 5

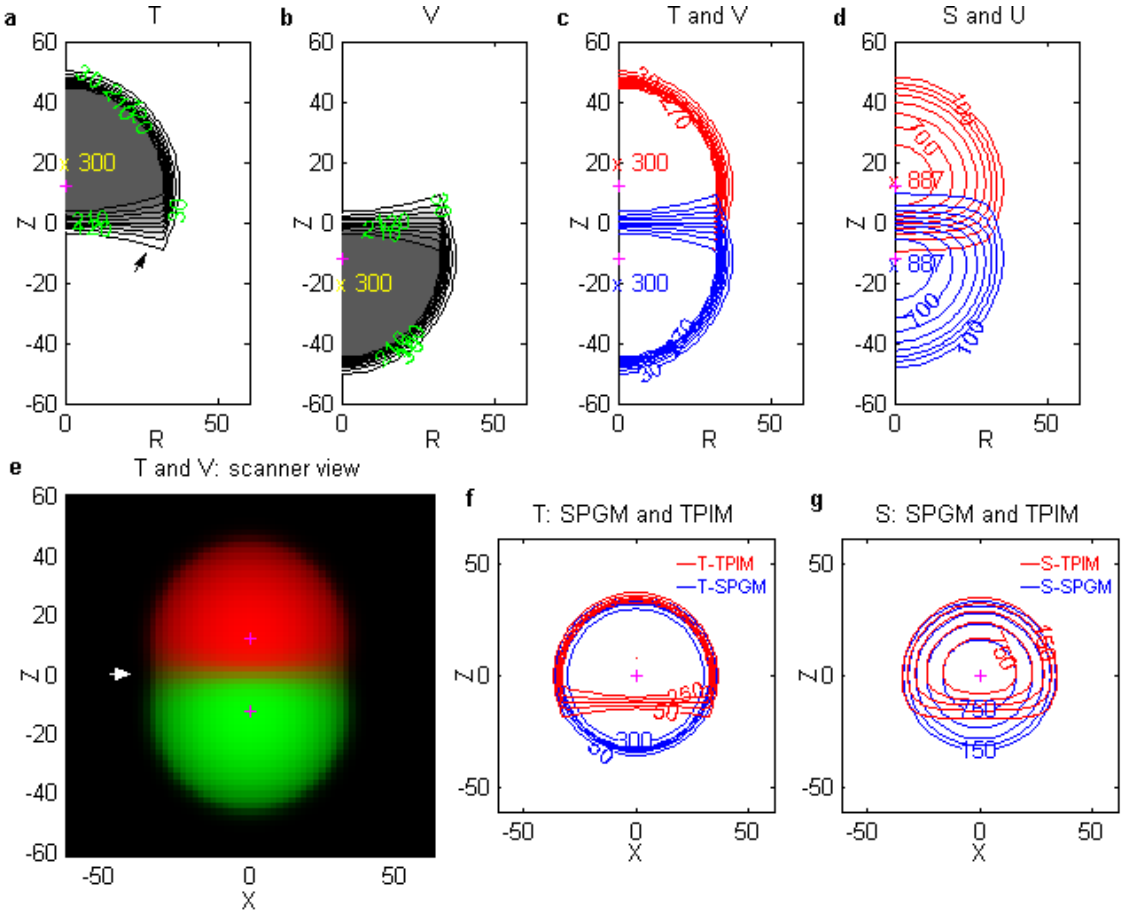
a
T
b
V
c
T and V
d
S and U
e
T and V: scanner view
f
T: SPGM and TPIM
T-TPIM
T-SPGM
g
S: SPGM and TPIM
S-TPIM
S-SPGM
R
Z
X

Figure 6

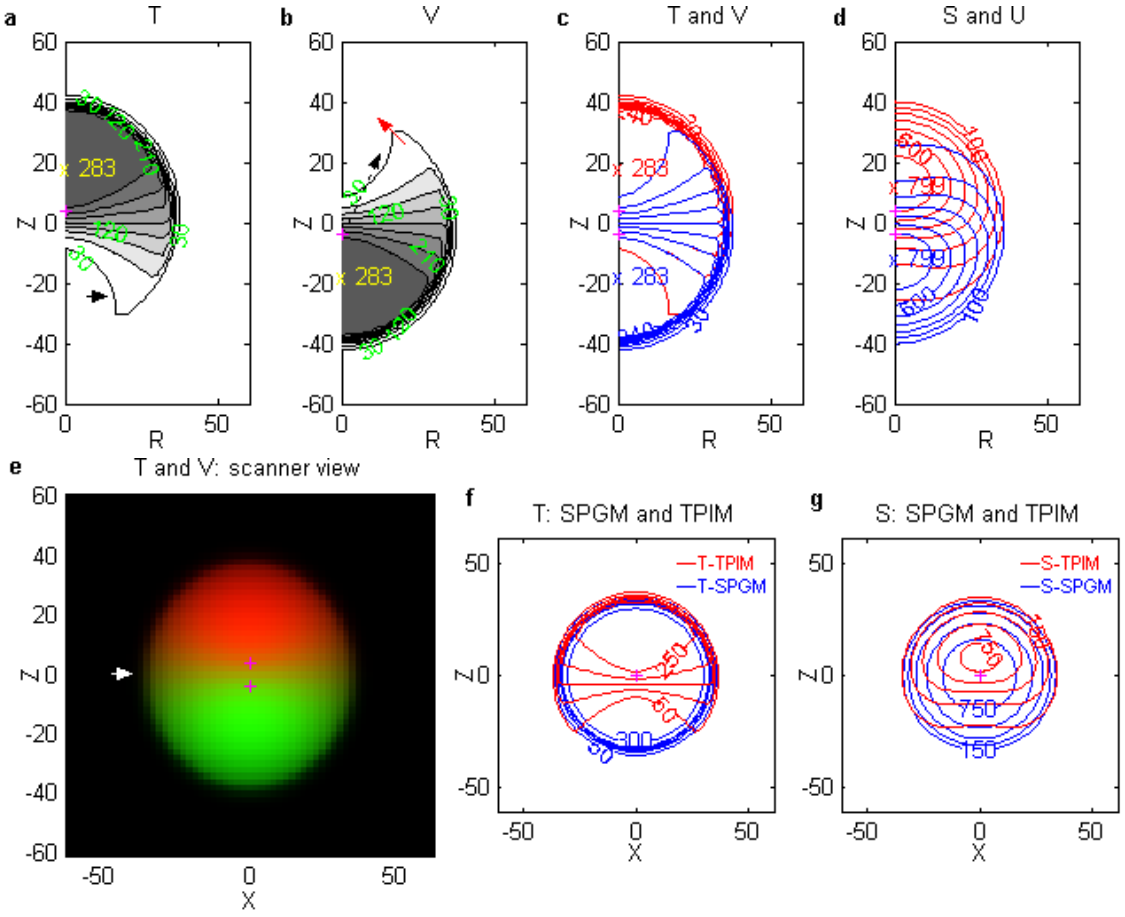
a
T
b
V
c
T and V
d
S and U
e
T and V: scanner view
f
T: SPGM and TPIM
T-TPIM
T-SPGM
g
S: SPGM and TPIM
S-TPIM
S-SPGM
R
Z
X

Figure 7

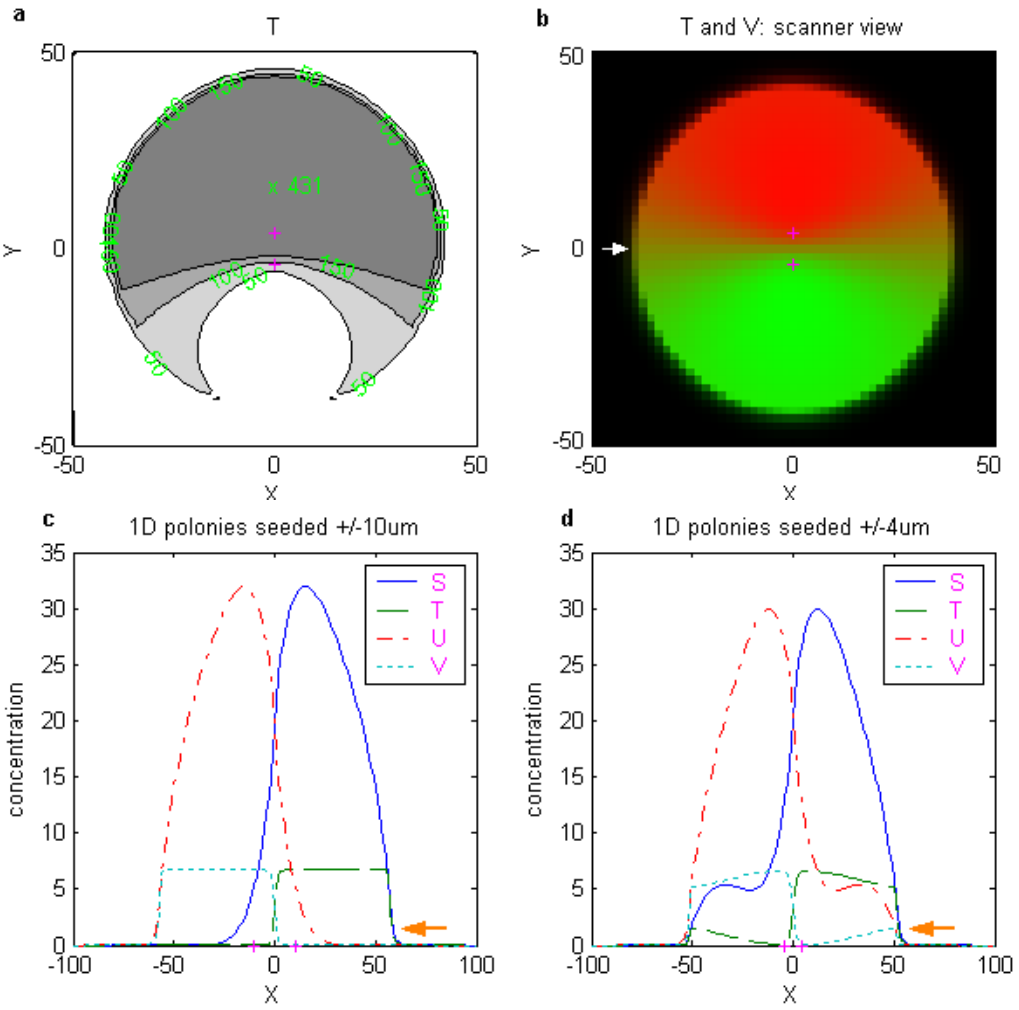
a
T
b
T and V: scanner view
c
1D polonies seeded +/-10um
d
1D polonies seeded +/-4um
concentration
X
Y
S
T
U
V

Figure 8

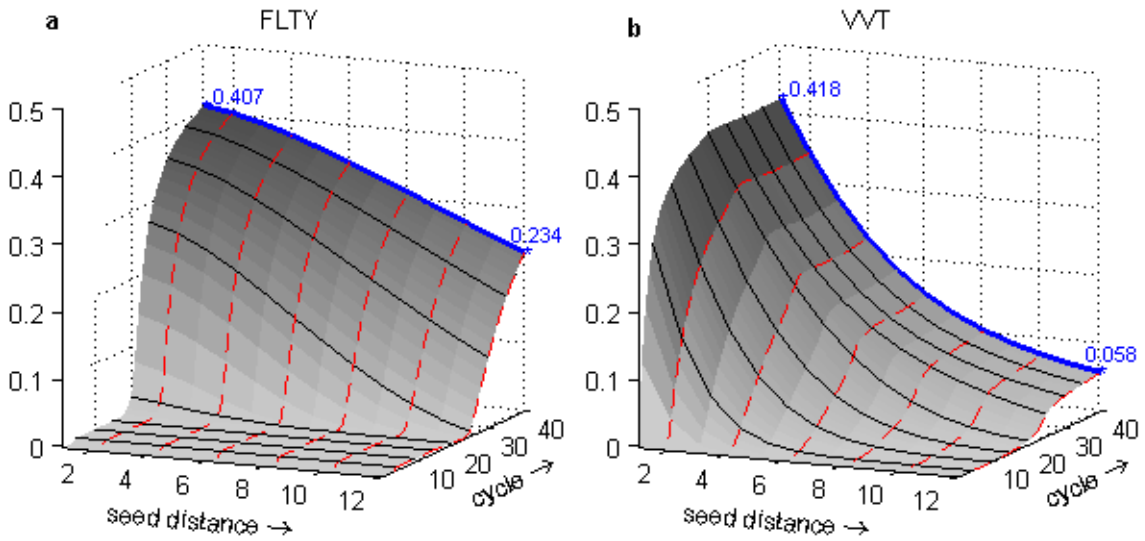
a
FLTY
0.407
0.234
0.5
0.4
0.3
0.2
0.1
0
2
4
6
8
10
12
seed distance →
10
20
30
40
cycle →
b
VVT
0.418
0.058
0.5
0.4
0.3
0.2
0.1
0
2
4
6
8
10
12
seed distance →
10
20
30
40
cycle →